

Supercritical Stability in a Sonar Receiver Circuit

Jonathan Tapson
Department of Electrical Engineering
University of Cape Town
Rondebosch, South Africa
jtapson@ebe.uct.ac.za

Abstract—We describe a simple circuit, inspired by the human auditory system, which allows controllable supercritical stability in a sonar receiver. The receiver is held on the threshold of self-oscillation when signal levels are low. The effect is to improve the sensitivity and SNR for small and subthreshold signals, at the cost of some bandwidth, while providing unchanged bandwidth and sensitivity at higher signal levels.

I. INTRODUCTION

The sensitivity and dynamic range of human and animal auditory systems is extremely impressive, and is believed to depend on highly localized electromechanical feedback at the level of the inner and outer hair cells of the cochlea [1, 2]. It has been suggested that the feedback maintains the forward (acoustic to electric) transduction mechanism in a state of supercritical stability [3-5]. Supercritical stability describes a system which is at the point of bifurcation from a single stable state to a bistable region, where the bifurcation is a Hopf bifurcation [6]. It is characteristic of this type of system that the transition is controllable and reversible. In the case of the auditory system, the bistable region would be one in which there was positive feedback, resulting in self oscillation and limit cycling. It is postulated that a sensory system held on the cusp of self oscillation would be most sensitive to subthreshold signals [4]. Some VLSI circuits approximating this type of mechanism have been implemented in silicon cochleas [7].

In this paper, we describe a circuit that implements this type of positive feedback in a sonar receiver, with dynamic adjustment to maintain supercritical stability. It is apparent that the effect is to alter the quality factor (Q) of the receiver. Signal receivers always represent a compromise between bandwidth and sensitivity. It is desirable to have a wide bandwidth for rapid response to transient inputs. However, a narrow bandwidth allows a better matched filter for noise rejection. The dynamical system created by this circuit acts to reduce the bandwidth and enhance the sensitivity (or increase the Q) at very low signal levels, while at higher signal levels the bandwidth is expanded (the Q is reduced).

The circuit is shown conceptually in Figure 1 and as a practical implementation in Figure 2.

Sonar topologies are discussed in Section IV. In all cases, the signal is encoded in the amplitude or phase of an acoustic or ultrasonic carrier. A receiver which enhances the SNR of carrier reception at low signal levels will improve the accuracy, and hence usefulness, of a sonar operating at extreme ranges.

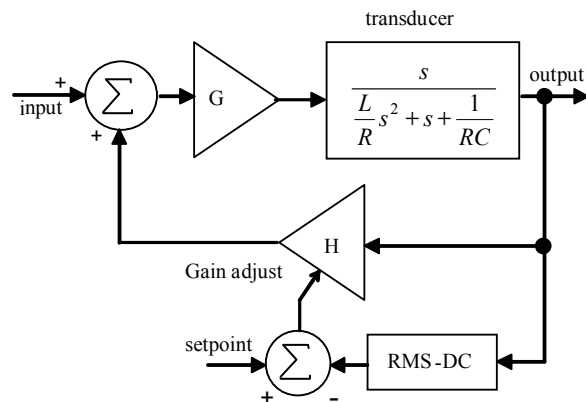


Figure 1. Block diagram of the circuit, showing inner feedback loop with positive feedback, and outer loop with gain adjustment. G and H are amplifiers; L, R and C are the parameters of the series (mechanical) LRC branch of the transducer.

II. OPERATION OF THE CIRCUIT

The present topology is intended for the standard type of piezoelectric transducer, which can be modeled as a series RLC resonant circuit in parallel with a capacitor representing the electrode capacitance.

The operation of the circuit is dependent on the level of signal received. This is measured using an RMS to DC converter, which measures the signal power at the output of the first amplification stage. The received signal is fed via a bandpass filter to a resistor/FET divider, which feeds back a

proportion of the signal to the other terminal of the transducer, as shown in Figure 2.

The inner loop of this circuit will be recognized as a Miller oscillator, in which the transducer acts as a series frequency-selective element [8]. The phase shift around the loop must be an integer multiple of 360° , and the impedances of the input and output elements attached to the transducer must be as low as possible. It would be equally straightforward to implement a Colpitts or Hartley oscillator, with the transducer as a parallel frequency-selective element.

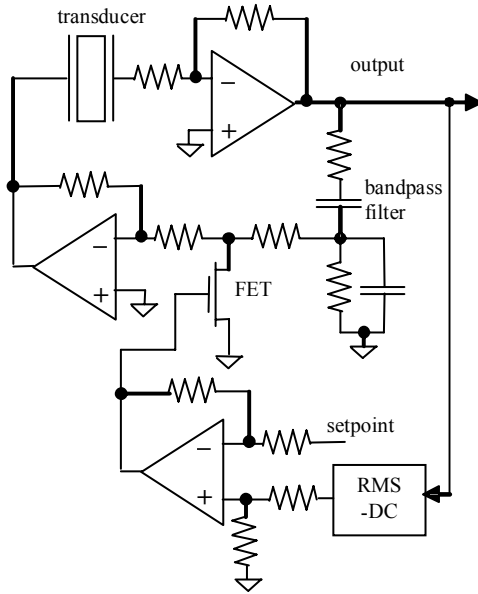


Figure 2. Circuit diagram, showing the transducer in place as a series frequency selective element. The bandpass filter is necessary as the real transducer has several resonant modes, and we desire the potential self-oscillation to be restricted to the frequency of transmission. The two inverting amplifiers give a total of 360° phase shift in the inside loop, assuming perfect amplifiers. The FET is able to short the feedback signal to ground, eliminating it entirely if the signal strength is sufficiently high.

This was avoided as the parallel arrangement would select for the parallel resonant frequency of the transducer, whereas the series resonance is more sensitive in receptivity; and the Colpitts oscillator is well known to have chaotic modes [9] which could confuse the analysis of this otherwise simple arrangement.

The gain of the feedback loop is adjusted by the output level of the RMS – DC converter. If the signal level is high, the feedback is completely disabled. In this case, the circuit reverts to being a simple open loop transducer amplifier such as is commonplace in sonar usage. If the signal level is below some set value, the proportion of feedback signal is increased from zero. At some level, which can be calculated analytically, using for example the Barkhausen criterion, or Routh-Hurwitz criterion, or a describing function, the system will start to oscillate. (The Barkhausen criterion [10] expresses the stability of a feedback loop in terms of the loop

gain and phase; the Routh-Hurwitz criterion [11] is an analytical method that derives stability in terms of the coefficients of the characteristic function of the loop; and a describing function [12] is an analytical approximation used to calculate the amplitude and frequency of limit cycling in nonlinear feedback loops). The setpoint should be adjusted so that this point is not reached, i.e. so that the circuit is on the threshold of oscillation when the signal level is that of noise only. Note that while the bifurcation point is mathematically exact, in practice the noise in the circuit has the effect of dithering the operational point back and forth across the bifurcation, so the system is less sensitive to setpoint adjustment than might be expected.

III. ANALYSIS

The circuit has two feedback paths. The bandwidths of operation of the two paths are separated by several orders of magnitude in frequency, so it is reasonable to model them independently. The inner loop can be reduced to the following transfer function:

$$\frac{y(s)}{x(s)} = \frac{Gs}{\frac{L}{R}s^2 + (1-GH)s + \frac{1}{RC}} \quad (1)$$

where $y(s)$ and $x(s)$ are output and input variables in the standard control systems usage. This has two expected features: it shows that the loop is unstable for $GH > 1$ (we have simply confirmed the Barkhausen criterion), and the frequency is determined by the usual expression $\omega = (LC)^{-1/2}$. It also suggests that the Q can be expressed as:

$$Q = \frac{\omega_o L}{(1-GH)R} \quad (2)$$

which suggests that the Q approaches infinity on the threshold of instability. There is a slow first-order loop which controls the size of H , and hence the limit cycle (oscillation) amplitude. Although it is not shown explicitly in the circuit diagram, the RMS-DC conversion involves an integration (governed by an averaging capacitor) which defines the bandwidth of the slow loop. If we make the reasonable approximation that the limit cycles are sinusoidal, the first order loop becomes linear, and we can use the describing function method [12] to analyze the second-order nonlinear loop. We can find a simple describing function for the limit cycles:

$$N(A, \omega) = \frac{4}{\pi A} (k - y_{rms}(t)) \quad (3)$$

where A is the limit cycle amplitude, k is the RMS setpoint, and $y_{rms}(t)$ is the actual RMS value. Solving the characteristic equation for the nonlinear loop (using the describing function method) gives $A = 4(k - y_{rms}(t))/\pi$ and once again the resonant frequency is $\omega = (LC)^{-1/2}$ – the frequency is defined by the resonance of the transducer, and the amplitude of the limit cycles by the desired minimum signal strength.

It should be noted that in the absence of negative feedback in the slow loop, oscillations in this system would grow until one of the active elements saturates, i.e. we would require a nonlinearity in the fast loop to limit the growth of oscillations. We have shown in a different context that a hard (step) nonlinearity in the fast feedback loop will achieve this. However, a step nonlinearity has the effect of exciting resonant modes of the sonar transducer which are outside the desired signal bandwidth, and has been avoided here for that reason.

The equivalence of the Barkhausen criterion and Hopf bifurcation conditions for LCR oscillators is implicit in most nonlinear analysis of feedback oscillators; it has been explicitly demonstrated by Ueta and Kawakami [13].

IV. RESULTS

The detection of an improvement in signal-to-noise ratio (SNR) at very low signal levels is not trivial. For the purposes of this study, we have assumed that an improvement in signal detection in a standard sonar application would constitute a useful result. There are several methods used for sonar ranging, which include the standard pulse-echo method, continuous-wave frequency modulation (CWFM), phase-lock ranging, and autocorrelation detection [14-17]. In pulse-echo and autocorrelation detection, the transmitted signal is pulsed or modulated in an on-off fashion (on-off keying, or OOK), and it is the pulses rather than the carrier signal that are detected. In CWFM and phase-lock ranging, the signal is transmitted continuously, and the frequency or phase of the carrier or the modulation is detected. We have used two methods of measuring the SNR. For the two ranging methods in which the signal is interrupted (using OOK), we have used the cross-correlation function between the transmitted and received signals as the measure of SNR (this is the fundamental process in autocorrelation ranging). For the two methods in which signal transmission is continuous, we have used coherence between the transmitted and received signals as the measure of SNR. Coherence is not as well-known a technique as cross-correlation; the coherence of two signals is defined as [18]:

$$\gamma_{XY}^2(f) = \frac{|G_{XY}(f)|^2}{G_{XX}(f)G_{YY}(f)} \quad (4)$$

where $G_{XY}(f)$ is defined in terms of the (single sided) cross-correlation function $R_{XY}(\tau)$:

$$G_{XY}(f) = 2 \int_{-\infty}^{\infty} R_{XY}(\tau) e^{-j2\pi\tau} d\tau. \quad (5)$$

In practice the integral is evaluated over twice the sample length and normalized in the usual way.

The slow outer feedback loop has a significant effect on signals which are pulsed on and off. When no signal is present, the feedback loop adjusts to maximize the feedback gain. This effectively increases the Q of the system, so that the sensitivity to a signal within the resonant band is higher, but the response to a transient change in signal amplitude is slower. When the signal is present with sufficient strength, the feedback is effectively disabled – shorted to ground through the FET as shown in Figure 2. This reduces the Q and improves the transient response. One effect is that the onset response (to an increasing signal) is slower than the offset response (to a reducing signal). This is evident in the cross-correlation results, where there is a loss of the expected symmetry with respect to the centre of the pulse. This can be seen to a small extent in Figure 4.

The results shown in Figures 3 and 4 were measured using a separate sonar transmitter and receiver, both of type Murata MA40B5S. These are small “bender” transducers intended for short-range measurement in air, and as such are not ideal for the purpose, having quite complex admittance characteristics. The transmitter was driven with a continuous 40kHz sinusoid for the data in Figure 3. This carrier was modulated with 50% OOK at a rate of 500Hz for the data in Figure 4.

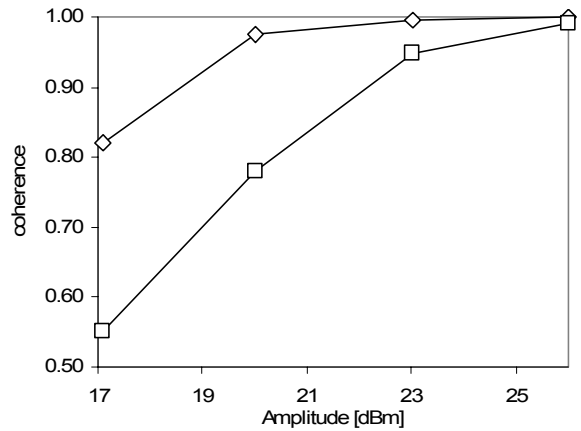


Figure 3. Coherence of received signals with respect to the transmitted signal. The squares indicate the performance with the receiver in the standard configuration, and the diamonds indicate the receiver in closed-loop supercritical stability. The horizontal units indicate power into the transmitter and are therefore somewhat arbitrary, as the received power depends on the range and reflectivity of the target.

V. CONCLUSIONS

We have described a circuit which can be used to keep a practical sonar transducer in a state of supercritical stability. The effect is to improve the sensitivity to signals which are of the same order of magnitude as the system noise. We conclude that the effect of the circuit is to raise the Q of the whole system at low signal levels, thereby narrowing the noise bandwidth at the expense of some loss of transient response. The circuit is suitable for use in both continuous-wave and pulsed sonar applications.

REFERENCES

- [1] T. Gold, "Hearing. II. The physical basis of the action of the cochlea.", *Proc. R. Soc. Lond. B: Biol. Sci.*, vol. 135, pp. 492-498, 1948.
- [2] Y. Choe, M.O. Magnasco and A.J. Hudspeth, "A model for amplification of hair-bundle motion by cyclical binding of Ca²⁺ to mechano-electrical-transduction channels", *Proc. Nat. Acad. Sci. USA*, vol. 95 (26), pp. 15231-15236, 1998.
- [3] V. M. Eguluz, M. Ospeck, Y. Choe, A. J. Hudspeth, and M. O. Magnasco, "Essential Nonlinearities in Hearing", *Phys. Rev. Lett.*, vol. 84, pp. 5232-5235, 2000.
- [4] S. Camalet, T. Duke, F. Jülicher and J. Prost, "Auditory sensitivity provided by self-tuned critical oscillations of hair cells", *Proc. Nat. Acad. Sci. USA*, vol. 97 (7), pp. 3183 - 3188, 2000.
- [5] A. Kern and R. Stoop, "Essential Role of Couplings between Hearing Nonlinearities", *Phys. Rev. Lett.* 91: 128101, (2003).
- [6] S.H. Strogatz, *Nonlinear Dynamics and Chaos*, Westview Press, Cambridge, 1994.
- [7] R. Sarpeshkar, R.F. Lyon and C.A. Mead, "An analog VLSI cochlea with new transconductance amplifiers and nonlinear gain control", *Proc. IEEE ISCAS '96*, pp. 292-296, 1996.
- [8] B. Parzen, *Design of Crystal and Other Harmonic Oscillators*, John Wiley and Sons, New York, 1983.
- [9] G.M. Maggio, O. De Feo and M.P. Kennedy, "Nonlinear Analysis of the Colpitts Oscillator and Applications to Design", *IEEE Trans. Circuits Syst. I*, vol. 36 (9), pp. 1118-1130, 1999.
- [10] H. Barkhausen, *Lehrbuch der Elektronenröhren - Elektronenröhren und ihre technischen Anwendungen*, S. Hirzel Verlag, Leipzig, 1923.
- [11] A. Hurwitz, "On the Conditions under which an Equation has only Roots with Negative Real Parts", in *Selected Papers on Mathematical Trends in Control Theory*, Ed. R. T. Ballman et al., Dover, New York, 1964.
- [12] J.-J.E. Slotine and W. Li, *Applied Nonlinear Control*, Prentice-Hall, New Jersey, 1991.
- [13] T. Ueta and T. Kawakami, "An aspect of oscillatory conditions in linear systems and Hopf bifurcations in nonlinear systems", *Proc. NDES2004*, Evora, Portugal, May 9-13, 2004.
- [14] C.D. Burnside, *Electronic Distance Measurement*, 3rd Ed., Blackwell Scientific Publications, Oxford, 1991.
- [15] P.T. Gough, A. de Roos and M.J. Cusdin, "Continuous transmission FM sonar with one octave bandwidth and no blind time", *IEE Proc. Part F*, vol. 131, pp. 270-274, 1984.
- [16] J. Tapson, "Wavemode Locking: A New Measurement Modality for Proximity Sensors", *Ultrasonics*, vol. 36, pp. 415-419, 1998.
- [17] H. Hamadene and E. Colle, "Optimal estimation of the range for mobile robots using ultrasonic sensors", *Proc. SICICA '97*, pp. 141-146, 1997.
- [18] J.S. Bendat and A.G. Piersol, *Engineering Applications of Correlation and Spectral Analysis*, John Wiley and Sons, New York, 1980.

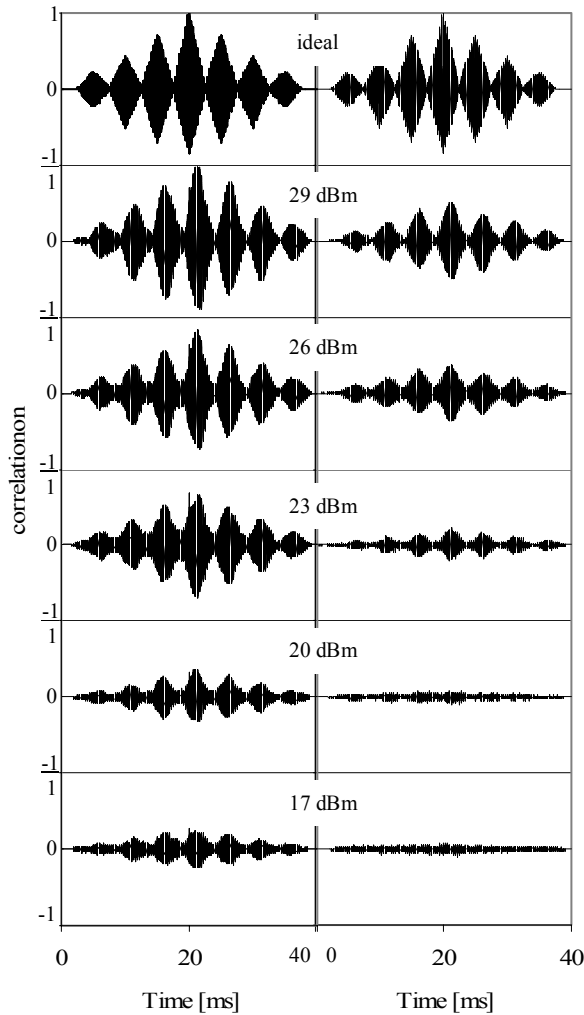


Figure 4. Cross-correlation waveforms for the supercritically stable (left) and standard (right) systems. Note that the real waveforms in both columns are offset slightly to the right, owing to the time of flight delay (this offset would be the measure of time of flight in autocorrelation ranging). The signal powers shown are for the transmitter, so they are shown only for a relative measure of signal strength.

It can be seen that the closed-loop (supercritically stable) system is substantially more coherent than the open-loop system, suggesting that the performance of phase-lock and CWFM sonars could be enhanced if this circuit was used.

Figure 4 shows the cross-correlation of the transmitted and received signals for discontinuous transmission. The closed loop system gives a higher degree of correlation, suggesting that results in pulse-echo and autocorrelation ranging modes will be more accurate with the use of the supercritically stable circuit.